Journal of Organometallic Chemistry 903 (2019) 120987

Contents lists available at ScienceDirect

Journal of Organometallic Chemistry

journal homepage: www.elsevier.com/locate/jorganchem

Ethylene oligomerization reactions catalyzed by homogeneous and silica immobilized N^O Fe(II) and Co(II) complexes

Arumugam Jayamani [a], George S. Nyamato [a, b], Stephen O. Ojwach [a, *]

[a] School of Chemistry and Physics, University of KwaZulu-Natal, Private Bag X01, Scottsville, Pietermaritzburg, 3209, South Africa
[b] Current Address: Department of Physical Sciences, University of Embu, P.O Box 6, Embu, 60100, Kenya

ARTICLE INFO

Article history:
Received 26 August 2019
Received in revised form
15 October 2019
Accepted 17 October 2019
Available online 18 October 2019

Keywords:
Iron
Cobalt
Homogeneous
Immobilization
Ethylene oligomerization

ABSTRACT

Treatment of 2-phenyl-2-((3(triethoxysilyl)propyl)imino)ethanol (**L1**) and 4-nitro-2-((3(triethoxysilyl) propyl)imino)methyl)phenol (**L2**) with MCM-41 support afforded the respective immobilized ligands (**L1im**) and (**L2im**). Reactions of synthons **L1**, **L2**, **L1im** and **L2im** with either $FeCl_2 \cdot 4H_2O$ or $CoCl_2$ led to the formation of their respective homogeneous and immobilized metal complexes [Fe(**L1**)$_2$] (**Fe1**), [Co(**L1**)$_2$] (**Co1**), [Fe(**L2**)$_2$] (**Fe2**), [Co(**L2**)$_2$] (**Co2**), [Fe(**L1im**)$_2$] (**Fe1im**), [Co(**L1im**)$_2$] (**Co1im**), [Fe(**L2im**)$_2$] (**Fe2im**), and [Co(**L2im**)$_2$] (**Co2im**). The compounds were characterized by FT-IR, NMR, ESI-MS, SEM-EDX and elemental analysis. Activation of the Fe(II) and Co(II) complexes with $EtAlCl_2$, resulted in active catalysts for the tandem ethylene dimerization and Friedel-Crafts alkylation of the toluene solvent to produce mainly alkyltoluenes. On the other hand, the use of chlorobenzene solvent and MAO co-catalyst led to the formation of mainly butenes. Generally, the immobilized catalysts exhibited lower catalytic activities, but with comparable selectivity to the homogeneous catalysts. Recycling studies established that the immobilized catalysts were active for three runs without loss of selectivity.

1. Introduction

Linear α-olefins are important feedstocks in the chemical industry that find widespread applications in various domains due to their capacity to undergo a number of transformations such as hydrogenation, hydroformylation, isomerization, oligomerization and polymerization [1,2]. Of notable example is ethylene oligomerization, which attracts considerable industrial interest due the production of higher olefins. These higher olefins are important intermediates to the manufacture of a variety of products such as detergents, polymers, lubricants, surfactants among others. Ethylene oligomerization can be carried out using homogeneous or heterogeneous catalysts and the product selectivity strongly depends on the type of catalyst and operating conditions [1]. Most of the current ethylene oligomerization commercial processes utilize homogeneous catalysts, such as trialkylaluminium (Chevron and Ethyl) and nickel complexes (Shell) [3–6].

Homogeneous catalysts have continued to attract considerable interest due to their high product selectivity. However, their industrial applications have been limited by the difficulty of separating the catalysts and products from the reaction mixture [7,8]. From an industrial viewpoint and indeed with respect to the green chemistry principles, heterogeneous catalysts provide numerous advantages over homogeneous analogues [1,9]. Of utmost importance is the ability to separate and re-use heterogeneous catalysts [10]. However, poor selectivity of the heterogeneous catalysts has also not left them without a setback. Thus, there are attempts to develop catalyst systems that possess the advantages of homogeneous catalysts (selectivity) and heterogeneous systems (separation). This attractive approach is loosely referred to as heterogenization of the homogeneous catalysts [11,12]. Different approaches have been used to develop efficient heterogenized systems such as encapsulation in zeolites [13,14], grafting on polymers [15,16] and immobilization in polysiloxane membranes [17]. Ordered mesoporous silica, for example, MCM-41 has attracted much attention, in the recent past, as solid support [18–21]. This is due to its high surface area, thermal and chemical stability in addition to shape selectivity [22].

We recently reported the application of both homogeneous [23] and heterogeneous [19] palladium(II) complexes bearing (phenoxy) imine ligand motifs in the methoxycarbonylation of olefins in which the complexes formed active catalysts to give predominantly linear esters. Encouraged by the performance of these catalysts in

* Corresponding author.
E-mail address: ojwach@ukzn.ac.za (S.O. Ojwach).

https://doi.org/10.1016/j.jorganchem.2019.120987
0022-328X/

the methoxycarbonylation of higher olefins, coupled with our continued pursuit for a catalytic system that combines the advantages of the homogeneous catalysts with those of heterogeneous processes, we herein report on ethylene oligomerization studies using homogeneous and immobilized Fe(II) and Co(II) catalysts chelated by (phenoxy)imine ligand. The effects of reaction conditions on ethylene oligomerization reactions, catalyst recycling and leaching have been studied and are herein reported.

2. Experimental section

2.1. Materials and instrumentation

All solvents were of analytical grade and were dried and distilled prior to use. The reagents (3-aminopropyl)triethoxysilane (97%), 2-hydroxy acetophenone (99%) and 2-hydroxy-5-nitrobenzaldehyde (98%) were purchased from Sigma-Aldrich; anhydrous $CoCl_2$ (98%) and $FeCl_2 \cdot 4H_2O$ (98%) were purchased from Merck and used as received without further purification. Ligands 2-phenyl-2-((3(triethoxysilyl)propyl)imino)ethanol (**L1**) and 4-nitro-2-((3(triethoxysilyl)propyl)imino)methyl)phenol (**L2**) and their respective MCM-41 immobilized systems (**L1im**) and (**L2im**)were prepared following our recently published procedures [19,23]. The infrared spectra were recorded on a PerkinElmer Spectrum 100 in the 4000−400 cm^{-1} range. TOF ESI-mass spectra were recorded on an LC premier micro mass spectrometer. GC analyses were performed on a Varian CP-3800 gas chromatograph equipped with a flame ionization detector and a 30 m (0.2 mm i.d., 0.25 μm film thickness) CP-Sil5 CB capillary column while GC-MS analyses were performed on a Shimadzu GC−MS-QP2010 fitted with a quadrupole mass detector. The Scanning Electron Microscopy (SEM) analyses and Energy Dispersive X-ray (EDX) spectroscopy were performed on a ZEISS EVO LS 15 scanning electron microscope.

2.2. Synthesis of homogenous and immobilized triethoxysilyl imino ligands

2.2.1. 2-Phenyl-2-((3-(triethoxysilyl)propyl)imino)ethanol (*L1*)

The ligand **L1** was synthesized as per the procedure reported in literature [19,23], by condensation of 2-hydroxyacetophenone (0.54 g, 4 mmol) and 3-APTES (0.8854 g, 4 mmol) in a dean stark set up using dichloromethane (15 mL) as solvent. The solvent from the reaction mixture was evaporated at the rotor evaporator to obtain yellow oily liquid and the analytical data obtained were identical with the report. Yield: 1.09 g (87%). ^{1}H NMR (400 MHz, $CDCl_3$, δ ppm): 7.53 (d, 1H, $^2J_{HH} = 8.0$ Hz, Ph-H), 7.30 (t, 2H, $^3J_{HH} = 7.8$ Hz, Ph-H), 6.94 (d, 1H, $^2J_{HH} = 7.40$ Hz, Ph-H), 6.76 (t, 1H, $^3J_{HH} = 7.2$ Hz, Ph-H), 3.86 (q, 6H, $^4J_{HH} = 7$ Hz, $C\underline{H}_2$−CH_3), 3.60 (t, 2H, $^3J_{HH} = 7.12$ Hz, $C\underline{H}_2$−N), 2.38 (s, 2H, $C\underline{H}_2$−OH), 1.91 (quint, 2H, $^5J_{HH} = 7.96$ Hz, −CH_2-$C\underline{H}_2$-CH_2-), 1.26 (t, 9H, $^3J_{HH} = 7$ Hz, $C\underline{H}_3$−CH_2), 0.79 (t, 2H, $^3J_{HH} = 8.28$ Hz, $C\underline{H}_2$−Si). ^{13}C{^{1}H} NMR (100 MHz, $CDCl_3$, δ ppm): 165.22 (-C=N), 132.57 (Ar−C), 127.93 (Ar-CH), 119.07 (Ar-CH), 116.48 (Ar-CH), 58.45 (-CH_2=N), 51.43 (-CH_2-CH_3), 23.94 (−CH_2−$C\underline{H}_2$-CH_2-), 18.31($C\underline{H}_3$−CH_2-), 8.19 (-CH_2-Si). IR ν_{max}/cm^{-1}: 2973 (ν OH), 1614 (ν C=N), 1071 (ν Si−O). ESI-MS: *m/z* (%) 338 (25%) [M^+].

2.2.2. 4-Nitro-2-(((3-(triethoxysilyl)propyl)imino)methyl)phenol (*L2*)

The ligand **L2** was obtained by following the above procedure of stirring 5-nitrosalicylaldehyde (0.67 g, 4 mmol) and 3-APTES (0.8854 g, 4 mmol) in dichloromethane (30 mL) for 12 h. Then the solvent from the reaction mixture is evaporated at the rotor evaporator to obtain yellow solid, which was then washed with dichloromethane, ether and dried. Yield: 0.84 g (54%). ^{1}H NMR (400 MHz, CDCl3, δ ppm): 8.35 (s, 1H, HC=N-), 8.25 (s, 1H, Ph-H), 8.20 (d, 1H, $^2J_{HH} = 9.32$ Hz, Ph-H), 6.95 (d, 1H, $^3J_{HH} = 9.32$ Hz, Ph-H), 3.86 (q, 6H, $^3J_{HH} = 7.0$ Hz, -$C\underline{H}_2$-CH_3), 3.70 (t, 2H, $^3J_{HH} = 6.8$ Hz, $C\underline{H}_2$−N), 1.90 (quint, 2H, $^5J_{HH} = 8.24$ Hz, −CH_2-$C\underline{H}_2$-CH_2-), 1.26 (t, 9H, $^3J_{HH} = 7.04$ Hz, $C\underline{H}_3$−CH_2), 0.71 (t, 2H, $^3J_{HH} = 8.36$ Hz, $C\underline{H}_2$−Si). ^{13}C{^{1}H} NMR (100 MHz, $CDCl_3$, δ ppm): 171.71 (-C=OH), 164.29 (-C=N), 137.96 (Ar−C), 128.91 (Ar-CH), 128.62 (Ar-CH), 120.09 (Ar-CH), 115.85 (Ar-CH), 59.05 (-CH_2=N), 58.57 (-CH_2-CH_3), 24.047 (−CH_2−$C\underline{H}_2$-CH_2-), 18.34 ($C\underline{H}_3$−CH_2-), 7.79 (-CH_2-Si). IR ν_{max}/cm^{-1}: 3068 (ν OH), 1609 (ν C=N), 1075 (νSi−O). ESI-MS: *m/z* 369 (100%) [M^+].

2.2.3. Immobilization *L1* with MCM-41(*L1im*)

To a suspended solution of MCM41 (0.25 g) in toluene (50 mL), ligand **L1** (0.5 g) was added and sonicated for 25 min. Then the reaction mixture was heated at 90 °C for 14 h. The resulting yellow precipitate was washed with ethanol and toluene to give pale yellow precipitate which was then dried in oven for 12 h at 100 °C. Yield: 0.61 g (81%). IR ν_{max}/cm^{-1}: 2944 (ν OH), 1614 (ν C=N), 1060 (ν Si−O).

2.2.4. Immobilization of *L2* with MCM-41(*L2im*)

The immobilized ligand ***L2im*** was obtained by following the above procedure using MCM-41 (0.20 g) and ligand **L2** (0.4 g) in 30 ml of toluene which obtained to obtain yellow precipitate. Then the obtained precipitate was washed with ethanol, dichloromethane, and toluene to give yellow solid after dried in oven for 2 h at 100 °C. Yield 0.47 g (78%) IR ν_{max}/cm^{-1}: 3072 (ν OH), 1611 (ν C=N), 1031 (ν Si−O).

2.3. Synthesis of homogeneous Fe(II) and Co(II) complexes

2.3.1. Synthesis of [Fe(*L1*)$_2$] (***Fe1***)

A methanol solution (10 mL) of **L1** (0.50 g, 1.5 mmol) was added dropwise to a methanol solution (10 mL) of $FeCl_2 \cdot 4H_2O$ (0.29 g, 1.50 mmol) and stirred overnight at room temperature. The resultant brown precipitate was then isolated by filtration, washed with diethyl ether to afford complex **1** as a brown powder. Yield: 0.49 g (62%). IR ν_{max}/cm^{-1}: 1632 ($\nu_{C=N}$), 1058 (ν_{Si-O}), 588 (ν_{Fe-O}). ESI-MS: *m/z* (%) 732.19 (47%) [M^+]. Anal. Calcd for $C_{34}H_{56}FeN_2O_8Si_2 \cdot H_2O$: C, 54.39; H, 7.79; N, 3.73. Found: C, 54.58; H, 6.93; N, 3.36.

The rest of the complexes were prepared following the procedure described for complex **Fe1**.

2.3.2. Synthesis of [Co(*L1*)$_2$] (***Co1***)

$CoCl_2$ (0.08 g, 0.60 mmol) and **L1** (0.42 g, 1.02 mmol). Bluish green powder. Yield: 0.26 g (52%). IR ν_{max}/cm^{-1}: 1626 ($\nu_{C=N}$), 1073 (ν_{Si-O}), 586 (ν_{Co-O}). ESI-MS: *m/z* (%) 735.28 (25%) [M^+]. Anal. Calcd for $C_{34}H_{56}CoN_2O_8Si_2$: C, 55.49; H, 7.67; N, 3.81. Found: C, 55.75; H, 7.16; N, 3.50.

2.3.3. Synthesis of [Fe(*L2*)$_2$] (***Fe2***)

$FeCl_2 \cdot 4H_2O$ (0.06 g, 0.4 mmol) and **L2** (0.10 g, 0.40 mmol). A brown solid. Yield: 0.09 g (62%). IR ν_{max}/cm^{-1}: 3317 ($\nu_{OH(water)}$), 1659 ($\nu_{C=N}$), 1094 (ν_{Si-O}), 574 (ν_{Fe-O}). ESI-MS: *m/z* (%) 794.17 (45%) [M^+]. Anal. Calcd for $C_{32}H_{50}FeN_4O_{12}Si_2$: C, 48.36; H, 6.34; N, 7.05. Found: C, 48.01; H, 6.48; N, 6.86.

2.3.4. Synthesis of [Co(*L2*)$_2$] (***Co2***)

$CoCl_2$ (0.04 g, 0.4 mmol) and **L2** (0.11 g, 0.40 mmol). Dark green powder. Yield: 0.096 g (64%). IR ν_{max}/cm^{-1}: 3386 ($\nu_{OH(water)}$), 1647 ($\nu_{C=N}$), 1094 (ν_{Si-O}), 575 (ν_{Co-O}). ESI-MS: *m/z* (%) 797.27 (57%) [M^+]. Anal. Calcd for $C_{32}H_{50}CoN_4O_{12}Si_2$: C, 48.17; H, 6.32; N, 7.02. Found: C, 48.39; H, 5.98; N, 7.37.

2.4. Synthesis of MCM-41 immobilized Fe(II) and Co(II) complexes

2.4.1. Synthesis of [Fe(**L1im**)$_2$] (**Fe1im**)

To a solution of $FeCl_2 \cdot 4H_2O$ (0.10 g, 0.50 mmol) in ethanol (20 mL), and ligand **L1im** (0.10 g) was added and refluxed overnight. The resultant pale brown precipitate was then isolated by filtration, washed with diethyl ether and dried in an oven at 110 °C to afford complex.

Fe1im as a brown solid. The percentage yield of the compound was calculated based on the recovered weight as a function of total mass of the reactants (metal salt and ligand). Yield: 0.13 g (65%). IR ν_{max}/cm^{-1}: 3287 (ν_{OH}), 1624 ($\nu_{C=N}$), 1039 (ν_{Si-O}), 560 (ν_{Fe-O}).

The rest of the complexes were prepared following the procedure described for complex **Fe1im**.

2.4.2. Synthesis of [Co(**L1im**)$_2$] (**Co1im**)

$CoCl_2$ (0.06 g, 0.50 mmol) and **L1im** (100 mg). Pale violet powder. Yield (based on recovered weight): 0.096 g (58%). IR ν_{max}/cm^{-1}: 3245 (ν_{OH}), 1634 ($\nu_{C=N}$), 1035 (ν_{Si-O}), 573 (ν_{Co-O}).

2.4.3. Synthesis of [Fe(**L2im**)$_2$] (**Fe2im**)

$FeCl_2 \cdot 4H_2O$ (0.10 g, 0.5 mmol) and **L2im** (100 mg). Light brown powder. Yield (based on recovered weight): 0.14 g (70%). IR ν_{max}/cm^{-1}: 3366 (ν_{OH}), 1633 ($\nu_{C=N}$), 1027 (ν_{Si-O}), 566 (ν_{Fe-O}).

2.4.4. Synthesis of [Co(**L2im**)$_2$] (**Co2im**)

$CoCl_2$ (0.06 g, 0.50 mmol) and **L2im** (100 mg). Light green powder. Yield (based on recovered weight): 0.12 g (72%). IR ν_{max}/cm^{-1}: 3361 (ν_{OH}), 1653 ($\nu_{C=N}$), 1039 (ν_{Si-O}), 562 (ν_{Co-O}).

2.5. General procedure for ethylene oligomerization reactions

Ethylene oligomerization reactions were carried out in a 400 mL stainless steel Parr reactor equipped with a mechanical stirrer set at 500 rpm, temperature controller and an internal cooling system. In a typical experiment, the reactor was preheated to 100 °C *in vacuo* and cooled to room temperature. The appropriate amount of complexes (catalyst precursor) (10.0 μmol) was transferred into a dry Schlenk tube under nitrogen and toluene (20 mL) was added using a syringe. The required amount of $EtAlCl_2$ (1.8 M in toluene) co-catalyst (1.1 mL to give a ratio of Al/M ratio of 200) was then injected into the Schlenk tube containing the pre-catalyst to form the active catalytic system. The resultant solution was then transferred *via* a cannula into the reactor. An additional 10 mL of toluene solvent was also transferred *via* a cannula into the reactor giving a total volume of 30 mL. The reactor was then flushed three times with ethylene with 10 bar pressure at 25 °C and the reaction was started. After 1 h, the reactor was cooled to −10 °C using liquid nitrogen and excess ethylene vented off. After the reaction time, the reaction was stopped by cooling the reactor to −10 °C and excess ethylene vented off. An exact amount of heptane (0.1 mL) was added as an internal standard and the mixture was analyzed by GC and GC-MS. The mass of C_4 was calculated based on the ratio of the corresponding peaks to the *n*-heptane peak in the gas chromatogram. The catalytic activity was based on the mass of the oligomer fractions obtained.

2.6. Recycling experiments

Recycling experiments were performed in a stainless steel autoclave Parr reactor equipped with a temperature control unit, an internal cooling system and a sampling valve at a constant pressure of ethylene of 10 bar. In a typical experiment, the reactor was charged with the appropriate heterogeneous pre-catalyst (10 μmol) in 30 mL of dry toluene saturated with ethylene. The reactor was then purged with ethylene and the appropriate amount of $EtAlCl_2$ solution was added to obtain an aluminium to a metal ratio (Al: M) of 200. After 1 h of reaction time, the reaction was stopped, the mixture cooled and the products analyzed by GC. After the first reaction, the products were removed from the reactor using a cannula and the catalyst recycling experiment was carried out by adding another 20 mL of dry toluene and 1.4 mL of $EtAlCl_2$ after which the reactor was charged with 10 bar of ethylene.

3. Results and discussion

3.1. Synthesis of ligands and their Fe(II) and Co(II) complexes

The (phenoxy)imine ligands (**L1** and **L2**) were synthesized by condensation of 2-hydroxyacetophenone or 2-hydroxy-5-nitrosalicylaldehyde with (3-aminopropyl) triethoxysilane according to the procedures in previous reports [19,23]. The immobilized ligands **L1im** and **L2im** were prepared successfully from their respective homogeneous ligands **L1** and **L2** by reacting with MCM-41 as shown in Scheme S1. Reactions of the ligands with either $FeCl_2 \cdot 4H_2O$ or $CoCl_2$ at room temperature resulted in the formation of the corresponding bis(chelated) Fe(II) and Co(II) complexes in moderate yields (Scheme 1). The homogeneous ligands **L1** and **L2** were characterized by ^1H NMR and ^{13}C NMR spectroscopy (Figs. S1−S4).For example, in the ^1H NMR spectraum of compounds **L1** and **L2**, the CH_2 protons next to the imine nitrogen atom shifted downfield at 3.60 and 3.70 ppm in ligands **L1** and **L2**, respectively (Figs. S1 and S2). Similarly, the CH_2 protons present at the second position of the C=O group in 2-hydroxy acetophenone slightly shifted up-field from 2.67 to 2.38 ppm for ligand **L1,**establishing the formation of C=N bond. We also observed an up-field shift in the aldehyde proton (H−C=O group) in 2-hydroxy-5-nitrobenzaldehyde from 10.84 ppm to 8.34 ppm prior to the formation of the imine group (H−C=N) in ligand **L2**. The ligands and their corresponding homogeneous metal complexes (**Fe1**, **Co1**, **Fe2** and **Co2**) were characterized by FT-IR spectroscopy, mass spectrometry and elemental analyses (Figs. S5−S8). The ESI mass spectra of the ligands, Fe(II) and Co(II) complexes showed various fragments that were attributed to the proposed compounds. For example, the molecular ion of complex **Fe1** showed a molecular ion peak at 732 amu, while the spectrum of **Co1** exhibited a molecular ion peak at 735 amu, consistent with the proposed structures in Scheme 1. FT-IR spectroscopy was also useful in the structural elucidation of the Fe(II) and Co(II) complexes. General shifts in wavenumbers upon coordination to the Fe(II) and Co(II) metal centres, consistent with literature precedence were observed [24]. For instance, the $\nu_{(C=N)}$ signal in **L1** and complex **Fe1** were recorded at 1615 cm^{-1} and 1632 cm^{-1}, respectively (Fig. 1). It was further noted from the IR spectra of the compounds that the OH signal was absent, consistent with deprotonation of the O−H proton to form anionic ligands of **L1** and **L2**.

The structural characterization of the immobilized compounds (**L1im**, **L2im**, **Fe1im**, **Co1im**, **Fe2im** and **Co2im**) was also performed using FT-IR in addition to Scanning Electron Microscopy (SEM) and Energy Dispersive X-ray (EDX) spectroscopy. The FT-IR bending vibrations between 1306 cm^{-1} and 1365 cm^{-1} were assigned to the Si−O−Si bonds of the MCM-41 support and established a successful formation of the immobilized ligands **L1im** and **L2im** [25]. In addition, the shifts in the $\nu_{(C=N)}$ signals in ligand **L2im** and the corresponding complex **Co2im** from 1611 cm^{-1} to 1653 cm^{-1}, respectively, established successful coordination of **L1im** to the Fe metal atom to form **Fe1im** complex (Fig. 1). These results are similar to those reported by Bhunia et al. [26], for Co(II) complexes bearing 3-aminopropyl-triethoxysilane organic moiety, where shifts from 1643 cm^{-1} in the ligand to 1632 cm^{-1} in the

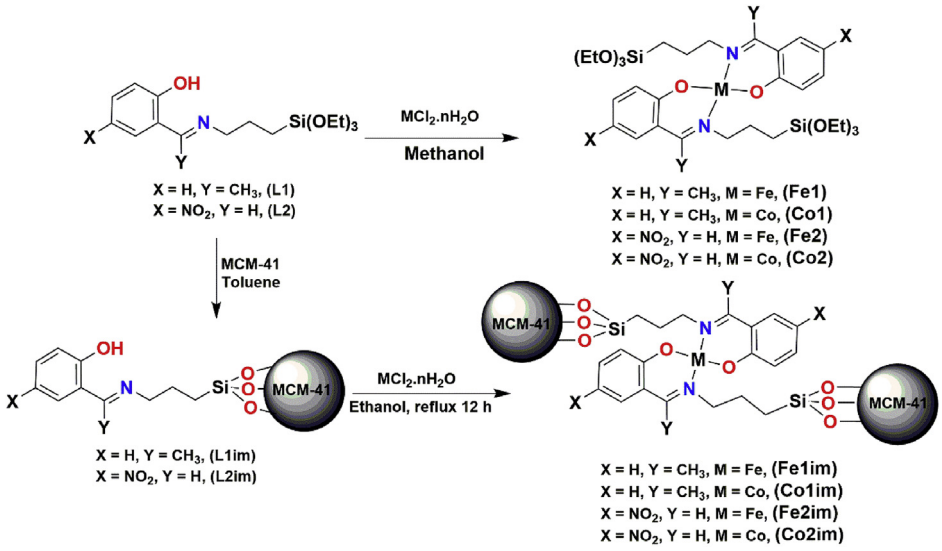

Scheme 1. Synthesis of homogeneous and MCM-41 immobilized Fe(II) and Co(II) complexes.

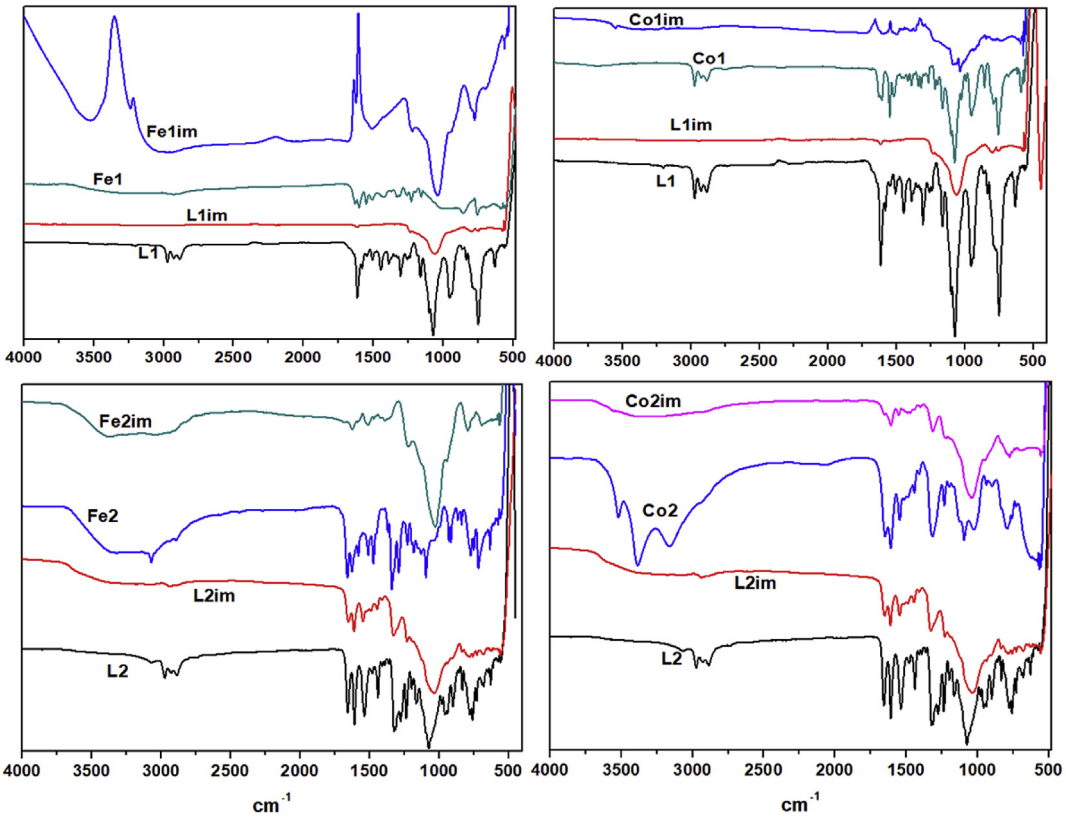

Fig. 1. FTIR Spectra of Schiff's base ligands, with their immobilized ligands and corresponding Fe(II) and Co(II) complexes.

complex were reported.

Scanning electron microscopy (SEM) and energy-dispersive X-ray spectroscopy (EDX) were used to study the morphology of the immobilized Fe(II) and Co(II) complexes. It is clear from Fig. S9 that the immobilized ligands and complexes exhibit undefined morphology with highly irregular shapes and sizes, with an agglomeration of particles, usually observed when MCM-41 is used as a support material [26]. The SEM images of complexes **Fe2im** and **Co2im** were more crystalline than those of the corresponding **Fe1im** and **Co1im** complexes, alluding to the possibility of ligand influence in breaking up of the MCM-41 crystal during sonication. The EDX analysis showed the presence of C, O, N, Si, Cl and Fe/Co in all the complexes and confirmed that the metal complexes were successfully immobilized on the silica surface (Fig. S10). The weight percentage of Fe(II) was observed to be higher than that of Co(II) in their respective complexes for both ligands. This is can be attributed to better interaction of Fe(II) with silica as opposed to Co as shown in Table 1.

Table 1
The EDX data for the immobilized complexes showing elemental compositions.

Element	Fe1im		Co1im		Fe2im		Co2im	
	Weight %	Atomic %	Weight %	Atomic %	Weight %	Atomic %	Weight %	Atomic %
C	40.92	52.37	36.72	47.81	46.71	59.15	48.16	58.78
N	3.55	3.89	3.58	4.00	4.23	4.59	2.27	2.37
O	35.72	34.32	38.68	37.80	28.31	26.91	34.48	31.59
Si	13.05	7.14	14.38	8.01	11.63	6.29	11.52	6.01
Cl	2.56	1.11	3.59	1.58	3.67	1.58	2.14	6.01
Fe	4.20	1.16	–	–	5.46		–	–
Co	–	–	3.04	0.81	–	–	1.43	0.36
Total	100.00		100.00		100.00		100.00	

3.2. Ethylene oligomerization reactions catalyzed by homogeneous complexes

The homogeneous complexes **Fe1, Co1, Fe2 and Co2** were investigated as pre-catalysts in the oligomerization of ethylene using $EtAlCl_2$ as co-catalyst in toluene solvent. In all cases, the complexes formed active catalysts for ethylene dimerization to give butenes, followed by *in situ* Friedel-Crafts alkylation of the toluene solvent by the butene oligomers to form butyltoluenes (Scheme 2). In addition, direct alkylation of the toluene solvent by the ethylene monomer to form ethyltoluenes was observed (Scheme 2). Detailed analyses of the oligomer products were carried out using GC and GC-MS (Figs. S11–S16). The Friedel–Crafts alkylation of toluene solvent used in the oligomerization of ethylene using $EtAlCl_2$ as a co-catalyst is not new and has been widely reported by us and other researchers [2,27–34]. The significant import of this data is that the current systems are predominantly ethylene dimerization catalysts. The presence of butenes, ethyltoluenes and butyltoluenes (Scheme 2) indicated that both partial alkylation of toluene solvent by the pre-formed oligomers and competitive ethylene oligomerization with direct alkylation of ethylene monomer are evident [34]. Table 2 shows a summary of the data obtained for all the pre-catalysts. In order to confirm the selective dimerization of these catalysts, further oligomerization reactions were run using complexes **Fe1** and **Co1** and $EtAlCl_2$ co-catalyst in chlorobenzene and hexane solvents instead of toluene (Table 2, entries 7-10). Significantly, no evidence of alkylation products was detected and butenes (76%-92% terminal butenes) were the only products (Fig. S12). Similar results have also been reported for 2-benzoimidazolyl-8-arylimino-5,6,7-trihydroquinoline-cobalt(II) chloride complexes with MAO co-catalyst [35]. The use of MAO as a co-catalyst with complexes **Fe1** and **Co1** further confirmed the dimerization of ethylene to form mainly terminal butenes (Table 2, entries 11 and 12). This supports the assertion that the more acidic $EtAlCl_2$ co-catalyst was largely responsible for the alkylation reactions observed [34].

Having established the efficacy of these pre-catalysts in initiating tandem ethylene dimerization and Friedel-Crafts alkylation reactions, we then examined the influence of complex/ligand structure in controlling both the catalytic activity and selectivity.

Table 2
Ethylene oligomerization data for homogeneous complexes **Fe1, Co1, Fe2** and **Co2**.[a]

Entry	Catalyst	Time (h)	Yield (g)	Activity[b]	C_4(α- C_4)	% Product Distribution			
						A	B	C	D
1	**Fe1**	1	1.84	1.84	7	9	66	8	10
2	**Co1**	1	1.07	1.07	3	15	67	10	5
3	**Fe2**	1	1.31	1.31	7	9	64	12	8
4	**Co2**	1	0.97	0.97	5	12	69	11	3
5	**Fe1**	0.5	0.44	0.88	13	12	62	8	5
6	**Fe1**	2	2.46	1.23	2	11	66	9	12
7[c]	**Fe1**	1	1.96	1.96	>99(92)	–	–	–	–
8[c]	**Co1**	1	1.13	1.13	>99(97)	–	–	–	–
9[d]	**Fe1**	1	1.82	1.82	>99(72)	–	–	–	–
10[d]	**Co1**	1	1.18	1.18	>99(67)	–	–	–	–
11[e]	**Fe1**	1	1.61	1.61	>99(86)	–	–	–	–
12[e]	**Co1**	1	0.98	0.98	>99(88)	–	–	–	–

[a] Reaction conditions: Amount of catalyst, 10 μmol; solvent, toluene, 30 mL; pressure, 10 bar; temperature, 25 °C; co-catalyst, $EtAlCl_2$ (Al/Me = 200); solvent, toluene (30 mL).
[b] Activity (10^5 g mol^{-1} h^{-1}).
[c] Reaction in chlorobenzene solvent. [d]Reaction in hexane solvent.
[e] Co-catalyst, MAO in toluene (Al/M = 200).

From the results in Table 2, it is interesting to note that the Fe(II) complex (**Fe1**) ligated by ligand **L1** exhibited higher catalytic activity of 1.84×10^5 g mol^{-1} h^{-1} compared to 1.31×10^5 g mol^{-1} h^{-1} obtained for complex (**Fe2**) ligated by ligand **L2** (Table 2, entries 1 and 3). From an electronic perspective, one would expect complex **Fe1** (bearing electron-donating methyl groups) to display lower catalytic activity due to reduced electrophilicity of the metal atom. In this instance, we can postulate improved stability of the resultant catalyst to account for its high catalytic activity. A similar observation has been made for a Ni(II) complex bearing *N*-(1-(pyridin-2-yl)ethylidene)-3-(triethoxysilyl)-1-propanamine ligand, whose better catalytic activity (566 kg mol Ni^{-1} h^{-1}) was ascribed to the methyl groups on the imine carbon, in contrast to the lower activity (374 kg mol Ni^{-1} h^{-1}) recorded by its analogous Ni(II) complex ligated by *N*-(2-pyridinylmethylene)-3-(triethoxysilyl)-1-propanamine [30]. We recorded a similar trend for the complexes **Co1** and **Co2**. In general, the Fe(II) complexes were more active than their Co(II) counterparts (Table 2). For example, complexes **Fe1** and

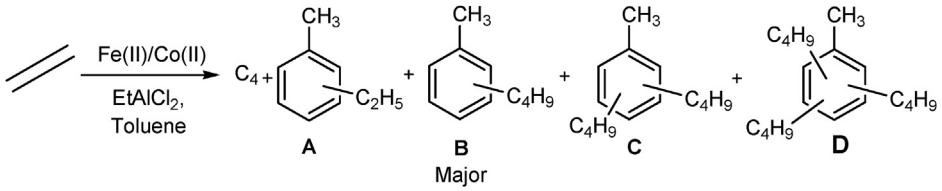

Scheme 2. Ethylene dimerization and Friedel-Crafts alkylation of toluene solvent by ethylene monomer and pre-formed butenes catalyzed by complexes **Fe1**, **Co1**, **Fe2** and **Co2** and $EtAlCl_2$ as co-catalyst.

Co1 demonstrated catalytic activities of 1.84×10^5 g mol^{-1} h^{-1} and 1.07×10^5 g mol^{-1} h^{-1}, respectively (Table 2, entries 1 and 2). This is consistent with our earlier observation [31] using unsymmetrical (pyrazolylmethyl)pyridine Fe(II) and Co(II) complexes, where catalytic activities of 467 kg mol^{-1} h^{-1} and 280 kg mol^{-1} h^{-1} were recorded for the Fe(II) and Co(II) complexes, respectively. We did not observe any discernible dependence of the oligomer/Friedel–Crafts product distribution on the identity of the complexes. This could arise from the similar steric environments of the complexes.

The stability of the active species was also probed using complex **Fe1** by varying reaction times from 0.5 h to 2 h (Table 2, entries 1, 5 and 6). Increasing reaction time from 0.5 h to 1 h led to increased catalytic activities from 0.88×10^5 g mol^{-1} h^{-1} to 1.84×10^5 g mol^{-1} h^{-1}, respectively. However, a further increase to 2 h was marked by a decrease in catalytic activity to 1.23×10^5 g mol^{-1} h^{-1} (Table 2, entry 6), which may be attributed to catalyst degradation [36]. From Table 2, it was also evident that reaction time had an influence on product distribution. It is apparent that longer reaction time gave higher amounts of butyltoluenes and subsequent reduction in the amount of C_4 oligomers. This is consistent with increased alkylation of toluene solvent by the preformed butenes over time. For example, increasing reaction time from 0.5 h to 2 h resulted in a decrease in the percentage composition of C_4 from 13% to 2% and a gradual increase in the percentage compositions of butyltoluenes (Table 2, entries 1, 5 and 6).

3.3. Ethylene oligomerization reactions using immobilized Fe1im, Co1im, Fe2im and Co2im complexes

Having established that the homogeneous complexes form active catalysts in tandem ethylene dimerization and Friedel-Crafts alkylation reactions, we then investigated the ability of the immobilized Fe(II) and Co(II) complexes**, Fe1im, Co1im, Fe2im** and **Co2im** in ethylene oligomerization reactions using $EtAlCl_2$ co-catalyst in toluene solvent (Table 3). Generally, the catalytic activities of the immobilized catalysts were lower in comparison to their corresponding homogeneous complexes (Fig. 2). For instance, complexes **Fe1** and **Fe1im** recorded catalytic activities of 1.84×10^5 g mol^{-1} h^{-1} and 0.97×10^5 g mol^{-1} h^{-1}, respectively (Fig. 2). The lower catalytic activity of the immobilized complexes may be assigned to steric crowding around the metal center that limits accessibility of ethylene monomer to the active metal atom [37,38]. Another plausible argument could be the low solubility of the immobilized systems as compared to their homogeneous analogues, hence limiting interaction between dissolved ethylene monomer and the active species [37]. This observation is consistent with previous reports of Rossetto et al. [39], in ethylene oligomerization reactions using MCM-41 immobilized nickel–β–diamine complexes. In another study, Kumar et al. [30] also reported reduced catalytic activities of the (imino)pyridine Ni(II) complexes immobilized on MCM-41.

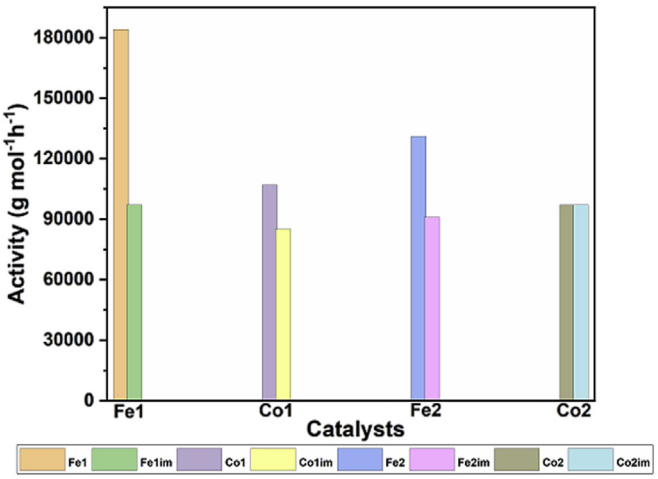

Fig. 2. A comparative profile of homogeneous and heterogeneous complexes.

With respect to selectivity, the immobilized complexes showed similar product distributions to the homogeneous catalysts to afford mainly alkyltoluenes (Table 3). This showed that immobilization of the homogeneous complexes did not significantly alter the selectivity of the resultant active species; a key attribute of immobilization of single site systems. The one outstanding difference is that the immobilized catalysts appeared to produce more of the dibutyltoluenes, while the homogeneous catalysts gave more mono-alkylated butyltoluenes (Table 2, entries 1-4, Table 3 entries 1-4 and Fig. 3). This behavior, could be ascribed to the high Lewis acidity of the resultant catalysts due to the presence of MCM-41, thus favoring more alkylation reactions. Indeed the propensity of MCM-41 to promote alkylation reactions has been documented [7]. As reported for **Fe1** and **Co1** complexes, the use of chlorobenzene solvent afforded only butenes (Table 3, entries 9 and 10).

We further studied the thermal stability of the immobilized catalysts by varying the reaction temperature from 25 °C to 100 °C (Table 3, entries 1, 5 and 6). It was observed that increasing the reaction temperatures from 25 °C to 50 °C resulted in increased catalytic activities from 0.97×10^5 g mol^{-1} h^{-1} to

Table 3
Ethylene oligomerization data for immobilized complexes, **Fe1im, Co1im, Fe2im** and **Co2im,** using $EtAlCl_2$ as co-catalyst in toluene.[a]

Entry	Catalyst	T (°C)	Pressure (bar)	Yield (g)	Activity[b]	C_4(α- C_4)	% Product Distribution			
							A	B	C	D
1	**Fe1im**	25	10	0.97	0.97	–	24	5	52	19
2	**Co1im**	25	10	0.85	0.85	4	22	9	50	15
3	**Fe2im**	25	10	0.91	0.91	–	23	9	52	16
4	**Co2im**	25	10	0.74	0.74	5	22	12	48	13
5	**Fe1im**	50	10	1.40	1.40	1	18	11	53	17
6	**Fe1im**	100	10	1.14	1.14	3	10	14	55	18
7	**Fe1im**	25	20	2.08	2.08	5	13	12	54	16
8	**Fe1im**	25	30	1.79	1.79	3	18	14	50	15
9[c]	**Fe1im**	25	10	1.24	1.24	>99(94)	–	–	–	–
10[c]	**Co1im**	25	10	1.06	1.06	>99(98)	–	–	–	–

[a] Reaction conditions: Amount of catalyst, 10 μmol; solvent, toluene (30 mL); $EtAlCl_2$ co-catalyst (Al/M = 200); toluene; time, 1 h.
[b] Activity in units of 10^5 g mol^{-1} h^{-1}.
[c] Reaction in chlorobenzene solvent.

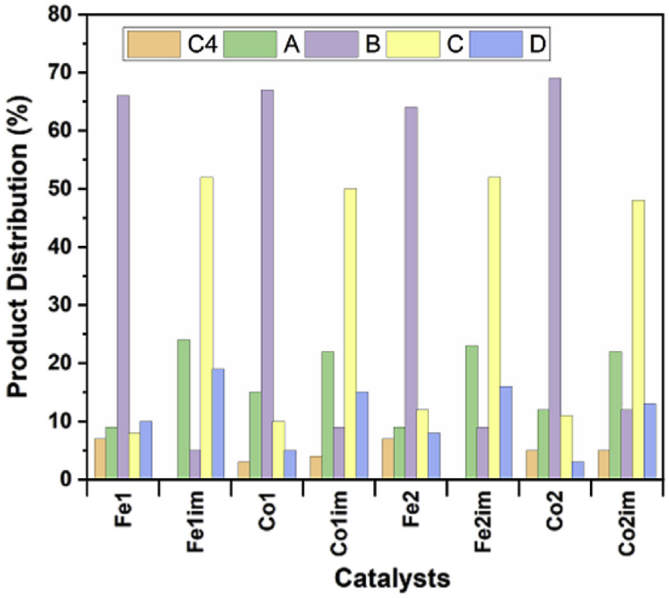

Fig. 3. A comparative profile of product selectivity of the homogeneous and immobilized Fe(II) and Co(II) complexes (see Scheme 2 for the identities of products **A**, **B**, **C** and **D**).

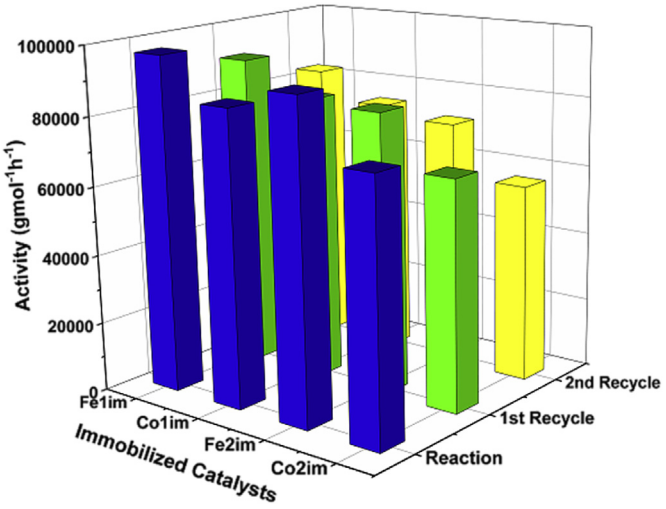

Fig. 4. Catalyst recycling experiments data. Reaction conditions: Amount of catalyst, 10 μmol (based on metal content); $EtAlCl_2$ co-catalyst (Al/M = 200); solvent, toluene, 30 mL; time, 1 h; temperature, 25 °C.

1.4×10^5 g mol^{-1} h^{-1} for pre-catalyst **Fe1im** (Table 3, entries 1 vs 5). On the other hand, a further increase of reaction temperature to 100 °C, resulted in a reduction in catalytic activity (Table 3, entries 1, 5 and 6), a feature which may be attributed to catalyst deactivation at higher temperatures. This trend mirrors those observed in the oligomerization of 1-hexene using mono-ligated (imino)pyridine Ni(II) catalysts where lower catalytic activities were obtained above 80 °C [40]. The effect of ethylene pressure on the catalytic performance of **Fe1im** was also studied by varying the pressure from 10 to 30 bar. As expected, increasing ethylene pressure from 10 bar to 20 bar resulted in increased catalytic activities from 0.97×10^5 g mol^{-1} h^{-1} to 2.08×10^5 g mol^{-1} h^{-1}, respectively (Table 3, entries 1, 7 and 8) [41]. Further increase in pressure to 30 bar, however, registered a decline in catalytic activity to 1.79×10^5 g mol^{-1} h^{-1} and this may be assigned to saturation limitations [30,36,42].

The reusability of heterogeneous catalysts is one of their central upsides over the homogeneous systems. We thus investigated the recovery and re-use of the immobilized pre-catalysts in ethylene oligomerization reactions (Fig. 4). This was done by recovering the catalyst from the products via filtration after the initial reaction and the subsequent batch was carried out by adding a fresh 20 mL of dry toluene and 1.4 mL of $EtAlCl_2$ without the addition of the pre-catalysts. The reactor was then charged with 10 bar of ethylene and reaction set at the prescribed pressure and temperature for 1 h. The results obtained confirmed the recyclability of the immobilized Fe(II) and Co(II) complexes as evidenced by the little reduction in catalytic activities in the first and second recycles (Fig. 4). More importantly, the product distributions remained the same, signifying retention of the nature of the active species during the three runs. In order to understand if leaching may be the reason for the slight reductions in the catalytic activities of the immobilized Fe(II) and Co(II) complexes in the second run, hot filtration test was conducted. This was done by adding 1.4 mL of $EtAlCl_2$ to the filtrate and subjecting the mixture to the typical catalytic conditions. Significantly, we did not observe any catalytic activity, confirming the absence of any leaching. Thus the observed marginal decline in catalytic performance could be attributed to partial decomposition or catalyst abrasion.

4. Conclusions

Homogeneous and silica immobilized N^O chelated Fe(II) and Co(II) complexes have been synthesized and structurally characterized. Activation of both the homogeneous and immobilized Fe(II) and Co(II) complexes with $EtAlCl_2$ as a co-catalyst resulted in the formation of active catalysts in tandem ethylene dimerization and Friedel–Crafts alkylation to give mainly alkyltoluenes (>90%) and small amounts of butene oligomers (<10%). On the other hand, the use of MAO as a co-catalyst resulted in the formation of predominantly butene oligomers (>99%). While the catalytic activities of the immobilized catalysts were lower than the homogeneous complexes, both systems displayed comparable product distribution. The immobilized catalysts were active in three runs without significant loss of catalytic activity and showed no leaching of the active species.

Declaration of competing interest

The authors declare no conflicts of interest with any other third party.

Acknowledgements

The authors would like to thank the University of KwaZulu-Natal and National Research Foundation – South Africa (Grant number: CPRR98938) for financial support.

Appendix A. Supplementary data

Supplementary data to this article can be found online at https://doi.org/10.1016/j.jorganchem.2019.120987.

References

[1] A. Finiels, F. Fajula, V. Hulea, Catal. Sci. Technol. 4 (2014) 2412–2426.
[2] R. Malgas-Enus, S.F. Mapolie, Inorg. Chim. Acta 409 (2014) 96–105.
[3] J. Skupinska, Chem. Rev. 91 (1991) 613–648.
[4] B. Cornils, W.A. Herrmann, M. Beller, R. Paciello, Applied Homogeneous Catalysis with Organometallic Compounds: A Comprehensive Handbook in Four Volumes, John Wiley & Sons, 2017.

[5] W. Keim, Angew. Chem. Int. Ed. 52 (2013) 12492–12496.
[6] A. Al-Jarallah, J. Anabtawi, M. Siddiqui, A. Aitani, A. Al-Sa'doun, Catal. Today 14 (1992) 1–121.
[7] E. Rossetto, B.P. Nicola, R.F. de Souza, K. Bernardo-Gusmão, S.B. Pergher, J. Catal. 323 (2015) 45–54.
[8] I. Kim, B.H. Han, J.S. Kim, C.-S. Ha, Catal. Lett. 101 (2005) 249–253.
[9] S. Bhunia, S. Koner, Polyhedron 30 (2011) 1857–1864.
[10] C. del Pozo, A. Corma, M. Iglesias, F. Sánchez, Organometallics 29 (2010) 4491–4498.
[11] K.P. Bryliakov, A.A. Antonov, J. Organomet. Chem. 867 (2018) 55–61.
[12] V. Hulea, ACS Catal. 8 (2018) 3263–3279.
[13] C. Bowers, P.K. Dutta, J. Catal. 122 (1990) 271–279.
[14] M. Salavati-Niasari, J. Mol. Catal. A Chem. 229 (2005) 159–164.
[15] I.J. Drake, K.L. Fujdala, A.T. Bell, T.D. Tilley, J. Catal. 230 (2005) 14–27.
[16] F. Minutolo, D. Pini, P. Salvadori, Tetrahedron Lett. 37 (1996) 3375–3378.
[17] I.F. Vankelecom, D. Tas, R.F. Parton, V. Van de Vyver, P.A. Jacobs, Angew. Chem. Int. Ed. 35 (1996) 1346–1348.
[18] D.E. De Vos, M. Dams, B.F. Sels, P.A. Jacobs, Chem. Rev. 102 (2002) 3615–3640.
[19] S.O. Akiri, S.O. Ojwach, Catalysts 9 (2019) 143.
[20] M.O. de Souza, L.R. Rodrigues, R.M. Gauvin, R.F. de Souza, H.O. Pastore, L. Gengembre, J.A. Ruiz, J.M.R. Gallo, T.S. Milanesi, M.A. Milani, Catal. Commun. 11 (2010) 597–600.
[21] M. Moorthy, A. Govindaraj, B. Madheswaran, B. Kannan, R. Rangappan, ChemistrySelect 1 (2016) 4833–4839.
[22] K. Parida, S. Singha, P. Sahoo, J. Mol. Catal. A Chem. 325 (2010) 40–47.
[23] S.O. Akiri, S.O. Ojwach, Inorg. Chim. Acta 489 (2019) 236–243.
[24] U.G. Singh, R.T. Williams, K.R. Hallam, G.C. Allen, J. Solid State Chem. 178 (2005) 3405–3413.
[25] G. Singh, A. Saroa, S. Khullar, S.K. Mandal, J. Chem. Sci. 127 (2015) 679–685.
[26] S. Bhunia, S. Jana, D. Saha, B. Dutta, S. Koner, Catal. Sci. Technol. 4 (2014) 1820–1828.
[27] M.K. Ainooson, S.O. Ojwach, I.A. Guzei, L.C. Spencer, J. Darkwa, J. Organomet. Chem. 696 (2011) 1528–1535.
[28] A. Budhai, B. Omondi, S.O. Ojwach, C. Obuah, E.Y. Osei-Twum, J. Darkwa, Catal. Sci. Technol. 3 (2013) 3130–3135.
[29] P.W. Dyer, J. Fawcett, M.J. Hanton, Organometallics 27 (2008) 5082–5087.
[30] K. Kumar, T. Godeto, J. Darkwa, J. Organomet. Chem. 818 (2016) 137–144.
[31] G.S. Nyamato, S.O. Ojwach, M.P. Akerman, J. Mol. Catal. A Chem. 394 (2014) 274–282.
[32] M. Yankey, C. Obuah, I.A. Guzei, E. Osei-Twum, G. Hearne, J. Darkwa, Dalton Trans. 43 (2014) 13913–13923.
[33] K. Song, H. Gao, F. Liu, J. Pan, L. Guo, S. Zai, Q. Wu, Eur. J. Inorg. Chem. (2009) (2009) 3016–3024.
[34] S.O. Ojwach, J. Darkwa, Catal. Sci. Technol. 9 (2019) 2078–2096.
[35] Y. Huang, R. Zhang, T. Liang, X. Hu, G.A. Solan, W.-H. Sun, Organometallics 38 (2019) 1143–1150.
[36] M.D. Doherty, S. Trudeau, P.S. White, J.P. Morken, M. Brookhart, Organometallics 26 (2007) 1261–1269.
[37] E. Rossetto, M. Caovilla, D. Thiele, R.F. de Souza, K. Bernardo-Gusmão, Appl. Catal. A-Gen. 454 (2013) 152–159.
[38] A.-M. Uusitalo, T.T. Pakkanen, E.I. Iskola, J. Mol. Catal. A Chem. 177 (2002) 179–194.
[39] E. Rossetto, B.P. Nicola, R.F. de Souza, S.B. Pergher, K. Bernardo-Gusmão, Appl. Catal. A-Gen. 502 (2015) 221–229.
[40] G. Song, L. Guo, Q. Du, W. Kong, W. Li, Z. Liu, J. Organomet. Chem. 858 (2018) 1–7.
[41] N. Zhang, J. Wang, H. Huo, L. Chen, W. Shi, C. Li, J. Wang, Inorg. Chim. Acta 469 (2018) 209–216.
[42] R.F. de Souza, K. Bernardo-Gusmão, G.A. Cunha, C. Loup, F. Leca, R. Réau, J. Catal. 226 (2004) 235–239.